SLAC-PUB--2809

DE82 005082

CRYSTAL BALL EVIDENCE FCR NEW STATES*

D. G. Coyne
(Representing the Crystal Ball Collaboration)[1]
Stanford Linear Accelerator Center
Stanford University, Stanford, California 94305
and
Princeton University, Princeton, New Jersey 08540

ABSTRACT

Evidence for three new particles observed in the Crystal Ball detector is presented. The first particle, at 3592 MeV, is seen inclusively in γ transitions from ψ', and is thus a candidate for η_c'. The other two, at 1440 and 1640 MeV, are best seen in exclusive decays of ψ involving a prompt γ, and are thus candidates for bound states of two gluons. Detailed reasons are presented to support the contention that these states are distinct from previously observed candidates such as E(1420). Alternative hypotheses are discussed.

I. INTRODUCTION

The search for new particles or states in data from the Crystal Ball has been concentrated in three sectors: (1) the detection of the remaining unseen members of the charmonium family below charm threshold, such as the $^1P_1$, η_c and η_c' (1^1S_o and 2^1S_o); (2) the search for new states X below the ψ which appear in $\psi \to \gamma X$, where X can include $q\bar{q}$ or gg resonances as well as more complex objects; (3) the search for states with open charm in the continuum above the ψ''. Of these three, the search for the gg states is clearly of greatest theoretical significance, but is also inherently most ambiguous experimentally. In this report, we present evidence for states found in categories (1) and (2), and show that the spin-parity analysis of the objects X lends some credibility to the gg hypothesis.

After a brief discussion of the detector, this report considers the candidate for η_c'. It then summarizes the findings on the two new states in $\psi \to \gamma X$. Because the interplay between theoretical prediction and experiment has been remarkably close for this chan-

* Supported in part by the Department of Energy, contract DE-AC03-76SF00515, and by National Science Foundation Grant PHY79-16461.

Presented at the Annual Meeting of the Division of Particle and Fields of the APS, Santa Cruz, CA, September 9 - 11, 1981.

nel, we then present a historical digression outlining this interplay. The report proceeds with an overview of the detailed analysis of the two new states. Finally, the theoretical interpretation and alternatives are explored.

II. THE DETECTOR

The Crystal Ball is a fieldless, segmented spherical shell of NaI(Tℓ) surrounding chambers having charged-particle tracking capabilities. The detector, built and operated by the Crystal Ball Collaboration,[1] is shown diagrammatically in Figure 1. A detailed description of the apparatus is given elsewhere;[2] for the purposes of this discussion there are several salient parameters.

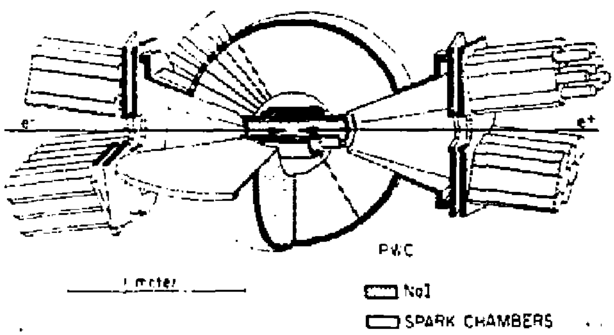

Fig. 1. Schematic cutaway view of the Crystal Ball Detector.

(a) The good energy resolution for photons is a well-known attribute of this instrument. At $E_\gamma = 100$ MeV, the error of $\sigma_E = \pm 4$ MeV is crucial for the inclusive observation of $\psi' \to \gamma\eta_c'$. Less well-known is the point that the energy resolution at $E_\gamma = 1000$ MeV, $\sigma_E = \pm 30$ MeV, is also crucial for inclusive observation of $\psi \to \gamma X$ if X is in the range 1-2 GeV.

(b) The Crystal Ball can overconstrain events for exclusive analysis. For an all-neutral final state (with the neutrals showering electromagnetically) we have a 3C fit -- the vertex position along the beams is an unknown. For additional nonshowering charged particles, one constraint (energy) is lost per particle but the vertex constraint is regained. One constraint is added for each intermediate mass (such as η or π^0) hypothesized to be present in the final state. Typical exclusive states from the Crystal Ball will be 2C, 3C and 5C. Combined with the angular resolution for γ (σ_{θ_γ} = 1 to 2°) and charged particles (σ_{θ_ψ} = .3 to 1°), the exclusive states often have substantially better mass resolution for the new particles than do the inclusive searches.

III. THE η_c' CANDIDATE

Following the discovery[3] of a candidate state for η_c in the inclusive γ spectra from ψ' and ψ, a further search for the transition $\psi' \to \gamma\eta_c'$ was made with the same Crystal Ball data. These data were subjected to refined pattern recognition cuts developed subsequent to that discovery. The familiar strong photon lines caused by transitions $\psi' \to \gamma\chi_{0,1,2}$ and $\chi_{1,2} \to \gamma\psi$ dominate the distribution. Small but statistically significant bumps appeared at photon energies of 638 MeV (the previous candidate for $\psi' \to \eta_c\gamma$) and at ~ 90 MeV. This latter peak motivated additional data runs at ψ' which brought the total number of ψ' produced in the detector to 1.78×10^6 (± 5%). Figure 2 shows the spectrum of inclusive photons from the additional data, which is abut 50% of the total. The effects mentioned recurred in the new data set. The insets show the background-subtracted fits to the total data sample. Table I

TABLE I
Parameters of η_c and η_c' candidates from inclusive fits.

	η_c	η_c'
$\langle E_\gamma \rangle$	638 ± 4 MeV	91 ± 1 MeV
M	2978 ± 4 MeV	3592 ± 5 MeV
Γ	12.4 ± 4.1 MeV	< 9 MeV (95% C.L.)
Significance	7σ	4.4 to 6.1 σ
BR($\psi' \to \gamma$ + state)	(.28 ± .08)%	(0.2-1.3)% (95% C.L.)

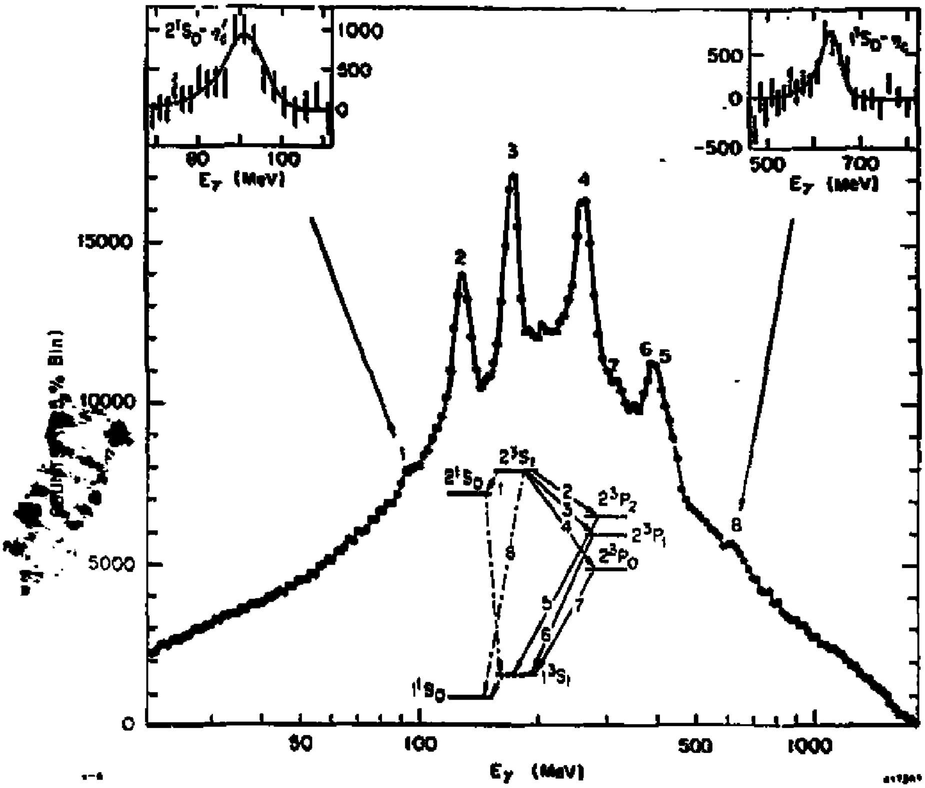

Fig. 2. Inclusive photon energy spectrum from $\psi' \to \gamma X$ for the most recent half of the data sample. Insets are the background subtracted signal from the entire data sample. The probable underlying term diagram is included.

summarizes the parameters of the states gleaned from these fits. Note that for the candidate $\eta_c'(3592)$ two types of background subtraction were performed. The inset shows the least restrictive technique, in which the background polynomial is allowed to attempt to fit the bump. Another method fits the background polynomial alone to the region excluding the peak (74-100 MeV) and then constrains the background to this result for the subtraction and subsequent peak-fitting. The statistical significance of the peak grows from 4.4 to 6.1 s.d. for this change in technique as expected if the background "robs" the peak in the former method. The natural full width at half-maximum for this state is not measureable with our resolution, but is < 9 MeV (95% C.L.) in either fit. This is in contrast to the η_c, where our best value from combined fits to ψ and ψ' is $\Gamma_{\eta_c} = 12.4 \pm 4.1$ MeV.

Given that this η_c' candidate seems statistically significant, the effect must be checked for the possibility that it is systematic. An investigation of such possibilities has been reported by Porter,[4] wherein details can be found establishing that

(1) There are no systematic effects in the spectra of charged particles, either real or fictitious, which can feed into the photon spectrum through the misidentification of a charged particle as a neutral.

(2) There are no obvious exclusive channels, such as $\psi' \to \pi^0\pi^0\psi$ or modes appearing in the γ-distribution through misidentification, which produce a spurious γ line at ~ 90 MeV.

(3) Checks to test for unknown systematics yield null results. These tests include a parallel identical inclusive analysis of ψ and also internal consistency checks on ψ' which look for the signal in data subsets divided with respect to geometry and time.

Our conclusion is that the η_c' candidate is fully on a par with the previous η_c candidate, insofar as the ψ' inclusive photons are concerned. It lacks the useful complementary evidence from an alternative spectrum (as for $\psi \to \eta_c\gamma$) and as of yet lacks totally exclusive final states which could confirm it and give quantum number determinations.

There has been one previous reference[5] to a possible η_c' state near this mass, measured in the cascade reaction

$$\psi' \to \gamma\eta_c' \quad ; \quad \eta_c' \to \gamma\psi \quad ; \quad \psi \to \ell^+\ell^-$$

The Crystal Ball cascade analysis,[6] while quite sensitive to suppressed reactions (such as $\psi' \to \pi^0\psi$), saw no evidence for η_c' in the cascades. Independently, we have now measured BR($\psi' \to \gamma + 3592$) =

0.2-1.3% (95% C.I.). The expected η_c' width (> 1 MeV) and the rate for $\eta_c' \rightarrow \gamma\psi$, obtained from scaling from our observed $\psi' \rightarrow \eta_c\gamma$, permit a determination of $BR(\psi' \rightarrow \gamma\eta_c')BR(\eta_c' \rightarrow \gamma\psi) < 10^{-5}$. This product is unobservable in any experiment done thus far. It does not appear that our present η_c' candidate is related to the former.

IV. NEW STATES FROM ψ DECAY

Two new states have emerged from the study of $\psi \rightarrow \gamma X$, with subsequent exclusive decay modes of X. We have named the two states $\iota(1440)$ and $\theta(1640)$. A list of the properties of these states as derived from Crystal Ball data is given in Table II.

TABLE II
New states from ψ decay.

Name	$\iota(1440)$	$\theta(1640)$
Mass	$1440 {+20 \atop -15}$ MeV	1640 ± 50 MeV
Γ (intrinsic)	$70 {+20 \atop -30}$ MeV	$220 {+100 \atop -70}$ MeV
J^{PC}	0^{-+} (99.99% C.L.)	2^{++} (95% C.L.)
Observed Decay Mode	$\iota \rightarrow \delta(980) + \pi$, $\delta \rightarrow K\bar{K}$	$\theta \rightarrow \eta\eta$
BR($\psi \rightarrow \gamma$ + state, state → observed decay)	(4.0 ± .7 ± 1.0) × 10^{-3}	(4.9 ± 1.4 ± 1.0) × 10^{-4}

These properties distinguish the states from previous ones of similar masses assigned to $q\bar{q}$ nonets. As such, the new states satisfy the minimal requirement to qualify as bound states of two gluons, but that assignment is not unique. We will discuss alternate choices.

Some scepticism is in order concerning gluonia candidates because of the large number and variety of (a) states available in particle spectroscopy and (b) gluonia states predicted by various theoretical models. In simple terms, the chance for coincidences is large. A good deal of our enthusiasm for these latest candidates stems from their appearance in a particular place judged a priori to be a possible cornucopia of gluonia states. We now digress to give a sketch of the history of such speculations.

Speculations on Gluonia

The following is not meant to be an exhaustive survey of all inputs to this subject, but should indicate at least the general course of events. The earliest reference to the idea of gluons bound to gluons occurred almost simultaneously with the concept of the non-Abelian group structure of the field quanta, long before QCD in its modern form emerged. A self-coupled gluon suggests gluon-only bound states, and references to such were made early by Nambu (1966), Fritzsch and Gell-Mann (1972), Wilson (1974) and many others,[7] in context with various theories. The first specific prediction for the two-gluon channel in ψ decays was made for the idealized case of completely noninteracting gluons by Chanowitz[8] (1975), who considered the process $\psi \to \gamma gg \to$ all hadrons. This was calculated as if the γgg were virtual and the γ disappeared in the final state, but the transition $\gamma gg \to$ hadrons was taken as unit probability. The effective result was the large branching ratio

$$\frac{\Gamma(\psi \to \gamma gg)}{\Gamma(\psi \to ggg)} = \frac{16}{5}\frac{\alpha}{\alpha_s} \approx 10\%$$

Okun and Voloshin[9] (1976) showed independently that the process $\psi \to \gamma gg$ should be identifiable by the unique spectral distribution of the real γ (Figure 3), which contains most of the rate at large $x = E_\gamma / \frac{1}{2} m_\psi$.

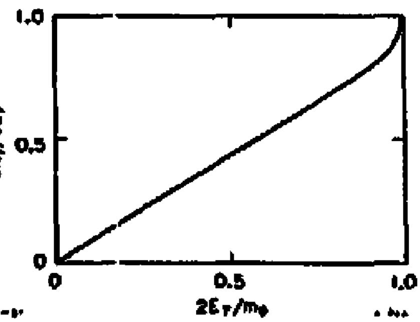

Fig. 3. The spectral distribution for the photon expected in $\psi \to \gamma gg$, with gluons massless and noninteracting.

The realization that the real γ could probe the gluon-gluon mass spectrum appeared in a work by Brodsky, et al.[10] (1977), where the x- and angular-distributions of the γ for noninteracting gg from Υ and $\psi \to \gamma gg$ were considered. [That the ψ is a likely place for such bound states to appear is clear from Figure 4. It shows that in the standard 3-gluon decay of ψ (a color singlet), any two gluons cannot be in a color singlet because they need to combine with the remaining gluon (a color octet) to form the ψ. In the process $\psi \to \gamma gg$, however, the gg are forced to be a singlet because the γ is colorless, and thus the γ potentially samples the gg mass spectrum of real particles.][11]

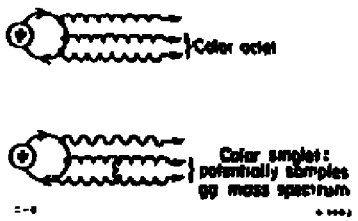

Fig. 4 Color combinations possible for two gluons in $\psi \to 3g$ and $\psi \to \gamma 2g$.

Brodsky made this explicit by showing how a gg resonance would appear in the inclusive γ spectrum (Figure 5). Even more speculatively, Koller and Walsh[12] (1977,1978) presented independent arguments that the high-x end of $\psi \to \gamma gg$ would be greatly suppressed and would consist largely of $\psi \to \gamma(q\bar{q})_{resonant}$ such as $\psi \to \gamma\eta$, $\gamma\eta'$, γf. At very low x they expected the prediction for γgg to be correct. At intermediate x they speculated that bound gg states could greatly distort and modulate the γ-spectrum. Figure 6 is derived from their earliest paper (the scales have been modified for comparison with Figures 3, 5, and 10). One must keep in mind that experimentally these photon signals will appear superposed on a much larger rapidly falling γ background from π^0 decays.

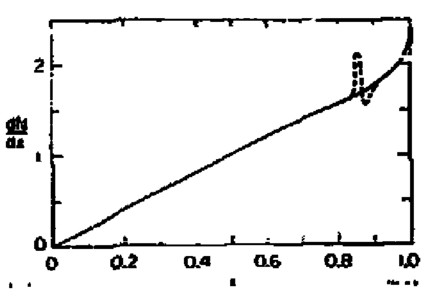

Fig. 5. Modulations of the inclusive γ energy spectrum in $\psi \to \gamma gg$ expected by resonances in gg.

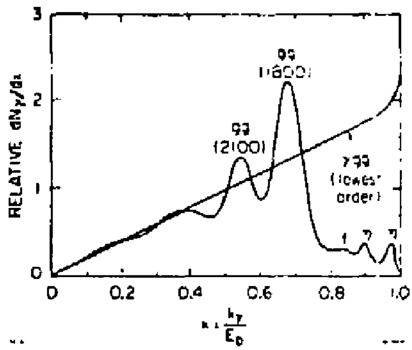

Fig. 6. A nonquantitative prediction of suppressions and modulations of the inclusive γ energy spectrum in $\psi \to \gamma gg$. Masses assigned to bumps are only to illustrate the approximate x-region and have no deeper significance. This plot is derived from the source, not reproduced.

A large number of predictions of various types has followed these early papers. One in particular (Bjorken 1979)[13] deserves mention, being as explicit a prediction as ever appears, given that it predicts an approximate mass, the best production and decay channels, the rate, the background and even the specific detector. We reproduce it here:

> "But an even more interesting question is what lies beyond. If narrow gluonium states dominate in the region from M = 1.4 GeV to M = 2 GeV, they should provide ~ 30% of all radiative decay modes. The γ-ray energies are 1 GeV, and probably badly buried in contamination from π^0 decays. A 2% γ-ray energy resolution corresponds to a resolution in gluonium mass of order 30 MeV. It may be unrealistic to try to resolve any gluonium lines by measurement of the recoil γ-rays alone -- even using Crystal Ball -- and reduction of background by looking for exclusive gluonium decay channels may be needed. Here one might try for some of those involving neutral decays, e.g., η. But it will be difficult. A scenario appropriate

for the Crystal Ball might be

$$\psi \to \gamma + \text{gluonium} \qquad 1/2\%$$
$$\hookrightarrow \eta + \eta \qquad 1\%$$
$$\hookrightarrow \gamma\gamma \;\; \hookrightarrow \gamma\gamma \qquad 38\% \times 38\% = 14\% \;. \quad (5.7)$$

The net signal is ~ 7 events/10^6 decays, even with a rather generous branching ratio assumed for the $\eta\eta$ decay-channel."

Initial Experiments on $\psi \to \gamma gg$

With this theoretical motivation, experimenters were looking for these specific features after each was predicted. J. S. Whittaker[14] (1976) first attempted to see the high-x peak in $\psi \to \gamma gg$ in the Mark I data, with an inconclusive result. Another attempt to measure the ψ end point spectrum was made by a small solid-angle, high resolution NaI detector at SPEAR (SP-27).[15] While no π^0 background subtraction was possible, it was shown (P. Moore 1978)[16] that the sharp high-x peak expected had not materialized. Figure 7 shows this result and indicates the equivalent limit $\alpha_s < 0.05$ (95% C.L.) that an unmodified theory would need to hide the effect in the π^0 tail above x = 0.8.

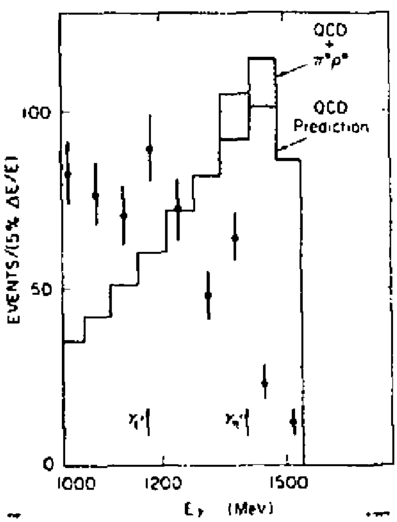

Fig. 7. The unsubtracted high-x end of the spectrum $\psi \to \gamma X$ (data points) (SP-27). The histogram is the lowest order QCD prediction with and without the process $\psi \to \pi^0\rho^0$ (which is indistinguishable from $\gamma\rho^0$). The arrows indicate where η' and f' would produce γ's, for the purposes of scale.

The first indication of a nonvanishing rate for $\psi \to \gamma gg$ came from the Lead-Glass Wall detector (Ronan, et al.,

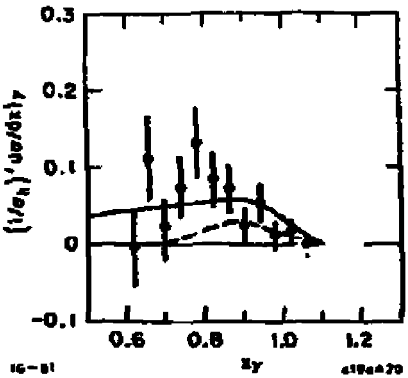

Fig. 8. The π^0-subtracted high-x end of the spectrum $\psi \to \gamma X$ (Lead-Glass Wall). The solid line is a fit to the lowest order QCD calculation, while the dashed line is that part of the rate attributable to known channels of ψ radiative decay.

1978).[17] Figure 8 shows the broad, indistinct signal after subtraction. The shape was deemed consistent with the theory, after large distortions by the poor-resolution shower detectors. The branching ratio was 2 to 6% ($0 < x < 1$). Evidence for a contribution over that previously measured for $\psi \to \gamma(q\bar{q})_{resonant}$ was cited. This result was quickly followed by a Mark II analogous measurement (Scharre, et al., 1979)[18]. Figure 9 shows that even with poor photon resolution, the greatly improved statistical precision rules out the high-x peak originally predicted in $\psi \to \gamma gg$. However, the branching ratio (3-5% above $x = 0.6$) is not in disagreement with theory. These two experiments showed that the prompt γ's exist, but that the simple QCD calculation had to be modified -- a conclusion easily accepted by theorists who were beginning to see large second-order corrections appear in related calculations.

When the Crystal Ball data on the π^0-suppressed high-x inclusive γ spectrum became available[19] (1979), it was clear that the prompt γ signal was rich in structure (Figure 10). Bumps were clearly visible at γ energies corresponding to radiative transitions to η, η', and $m = 1450$ MeV, with hints of effects elsewhere in

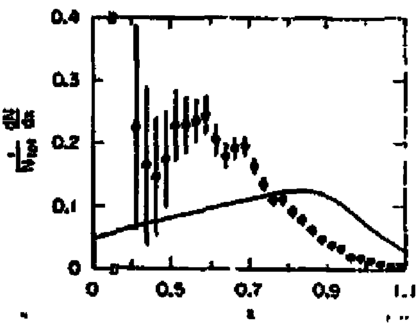

Fig. 9. As for Figure 8, except for Mark II data.

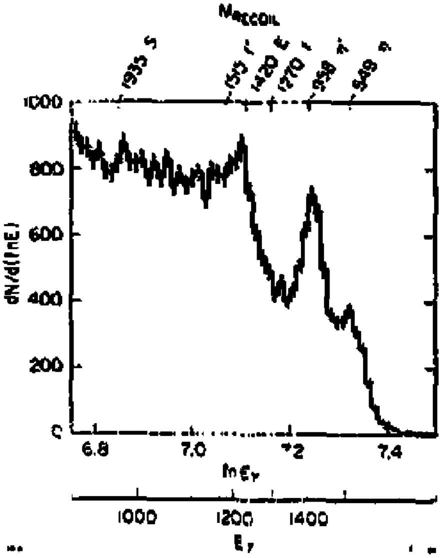

Fig. 10. The unsubtracted high-x end of the spectrum $\psi \to \gamma X$ from early Crystal Ball data (summer 1979). The particle names along the top of the graph serve as scale markers, not as assignments of hypotheses to bumps in the spectrum.

the spectrum. Work to find exclusive channels in ψ decay culminated in the detection by the Mark II (Scharre, 1979)[20] in $\psi \to \gamma K^{\pm} K_s^0 \pi^{\mp}$, by the Crystal Ball (Aschman, 1979)[21] in $\psi \to \gamma K^+ K^- \pi^0$ and possibly in $\psi \to \gamma \pi^+ \pi^- \eta$. Figure 11 shows the Mark II result, where the $K^{\pm} K_s^0 \pi^{\mp}$ clearly resonate near 1440 MeV, with a strong suggestion that $K\bar{K}$ are resonant at $\delta(980)$.

In response to these data, Chanowitz, Donoghue et al., and Ishikawa[22] (1981) have independently proposed that this reaction could be[23] $\psi \to \gamma(gg)_{1440}$ instead of $\psi \to \gamma E(1420)$, where $E(1420) \to K^* K$ has long been assigned to the $q\bar{q}$ 1^{++} nonet on the basis of its spin determination[24]. The crucial test (among others) is a spin-parity determination of the object seen in ψ decay.

The Crystal Ball detector has been taking more data at the ψ, roughly doubling the data sample — the total sample is now 2.17×10^6 ψ. We now continue with a discussion of the new states seen in these ψ decays.

Crystal Ball Results on $\psi \to \gamma\iota(1440)$

The updated Crystal Ball result for $\psi \to \gamma K^+ K^- \pi^0$ for the entire data sample is shown in Figure 12. The shaded events are those with $m_{K\bar{K}} < 1.125$ GeV, i.e., those likely to be associated with the tail of $\delta(980)$ (the central value of δ is below $K\bar{K}$ threshold). The

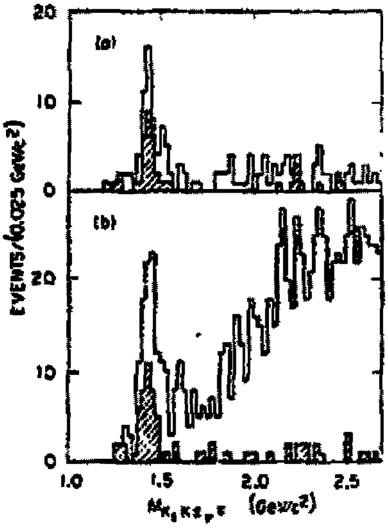

Fig. 11. The invariant $K_sK^{\pm}\pi^{\mp}$ mass spectrum from the reaction $\psi \to \gamma K_s K^{\pm}\pi^{\mp}$ (Mark II data). The spectrum with a detected γ is given in (a) and with no such restriction in (b). Crosshatched spectra correspond to a mass cut on $m_{K_sK^{\pm}}$ which selects $K_sK^{\pm}$ associated with $\delta(980)$.

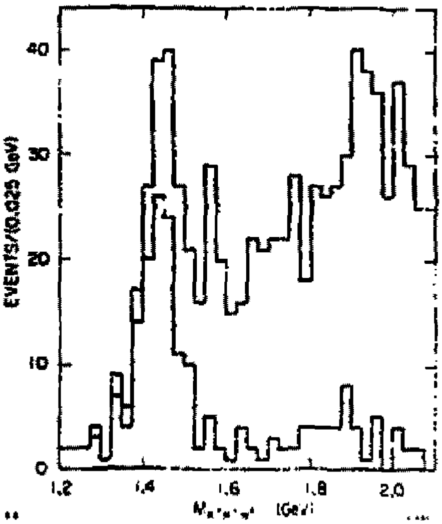

Fig. 12. The spectrum analogous to Figure 11 for the entire data sample from the Crystal Ball.

corresponding inclusive ι distribution is shown in Figure 13. The width of ι in the inclusive distribution should be dominated by the energy resolution on the γ, whereas the exclusive fit reduces the resulting error on m_{ι} to a negligible level compared to the natural width of 70^{+20}_{-30} MeV. Table III shows the comparison of these errors.

The ambiguity between $E(1420) \to K^*K$ and $\iota(1440) \to \delta\pi$ is illustrated by examining the Dalitz plot for this decay for $\iota(1440)$, Figure 14. Decay into K^*K would produce bands as shown, while decay into $\delta\pi$ would populate the region of $K\bar{K}$ masses from the kinematic boundary up to the $K\bar{K}$ mass cut chosen. The latter hypothesis looks more consistent with the data, but limited statistics and the proximity to the boundary of the K^* bands obscures the interpretation.

TABLE III

Resolutions for Inclusive and Exclusive $\psi \rightarrow \gamma X$.

		1	0
M_X		1440 MeV	1640 MeV
Γ_X		70 MeV	220 MeV
k_γ		1212 MeV	1113 MeV
σ_{k_γ}	(detector)	± 29 MeV	± 27 MeV
σ_{k_γ}	(induced by Γ_X)	± 16 MeV	± 59 MeV
σ_{M_X}	(in a single unfitted event)	± 62 MeV	± 51 MeV
σ_{M_X}	(in a single fitted event)	~ ± 20 MeV	~ ± 20 MeV

The ambiguity can be resolved by a complete partial wave analysis of these data. For added details of this analysis see Scharre.[25] The analysis is carried out using four coherent partial wave amplitudes together with a noncoherent phase space amplitude:

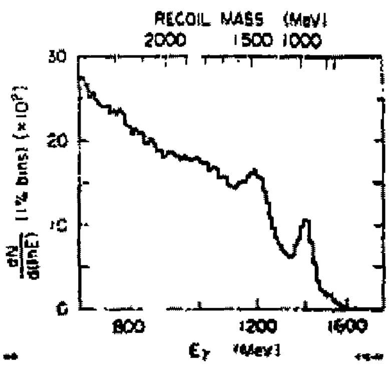

Fig. 13. The spectrum analogous to Fig. 10, but from the entire Crystal Ball data sample. Some background-suppressing cuts applied in Fig. 10 have not been used here.

$\psi \rightarrow \gamma X$

$X \rightarrow$	$K\bar{K}\pi$	(phase space)
	$\delta^0 \pi^0$	(spin 0)
	$K^* \bar{K} + \bar{K}^* K$	(spin 0)
	$\delta^0 \pi^0$	(spin 1)
	$K^* \bar{K} + \bar{K}^* K$	(spin 1) .

While these amplitudes do not exhaust all possibilities, they serve to clarify the likely alternatives. The result of

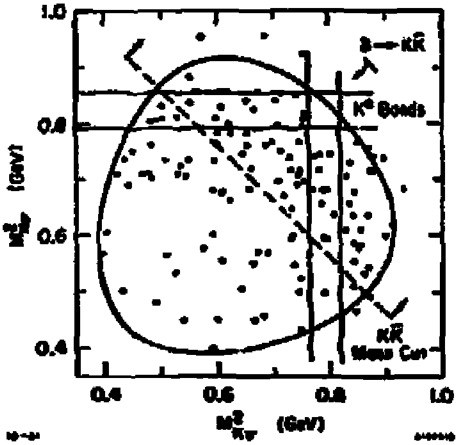

Fig. 14. The Dalitz plot for the decay $\iota \to K\bar{K}\pi$ for the total Crystal Ball data sample, with $1.4 < m_{K^+K^-\pi^0} < 1.5$ GeV.

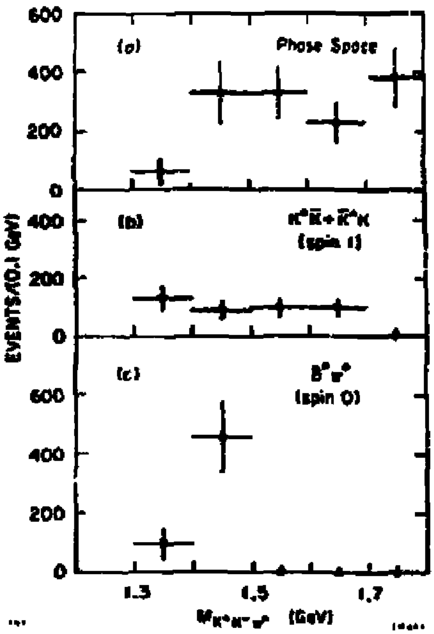

the fit to the data is shown in Figure 15, where the significant amplitudes are displayed. Only $\delta^0\pi^0$ (spin 0) shows any resonant form near the bump observed in $m_{K\bar{K}\pi}$. The total contribution of $K^*\bar{K} + \bar{K}^*K$ is less than 25% (90% C.L.) and is non-resonant. In order to gain a feeling for the relative probabilities of these amplitudes, if one amplitude (plus phase space) is to explain the distribution, fits were made

Fig. 15. The $m_{K^+K^-\pi^0}$ dependence of the surviving partial wave amplitudes for $\iota \to K\bar{K}\pi$ (Crystal Ball data).

with $\delta^0\pi^0$ (spin 0) and $K^*\bar{K} + \bar{K}^*K$ (spin 1) separately. The fits give the probability that $K^*\bar{K}$ (spin 1) can explain the data to be only 1% of that for the $\delta^0\pi^0$ (spin 0) hypothesis. Alternatively, if the amplitude is forced to be $\delta^0\pi^0$ + phase space, the probability for spin 1 is only 10^{-4} of that for spin 0. The competition among these hypotheses is illustrated by the m_{KK} and $m_{K\pi}$ Dalitz plot projections in the ι mass region (Figures 16 and 17) together with their

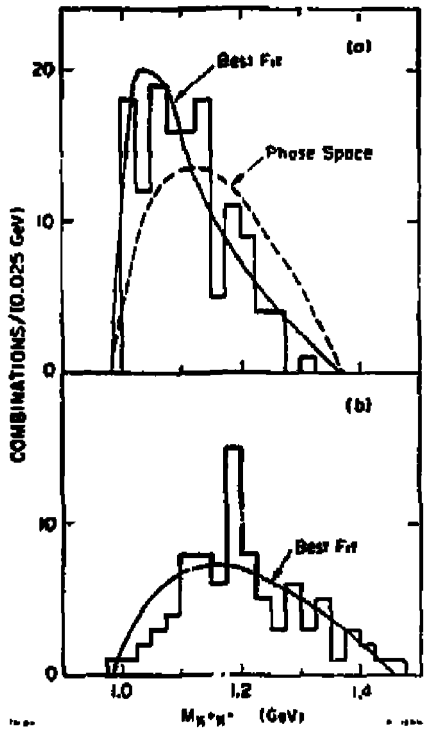

Fig. 16. Projections in $m_{K^+K^-}$ of the $K^+K^-\pi^0$ Dalitz plot for (a) $1.4 < m_{K^+K^-\pi^0} < 1.5$ GeV and (b) $1.5 < m_{K^+K^-\pi^0} < 1.6$ GeV.

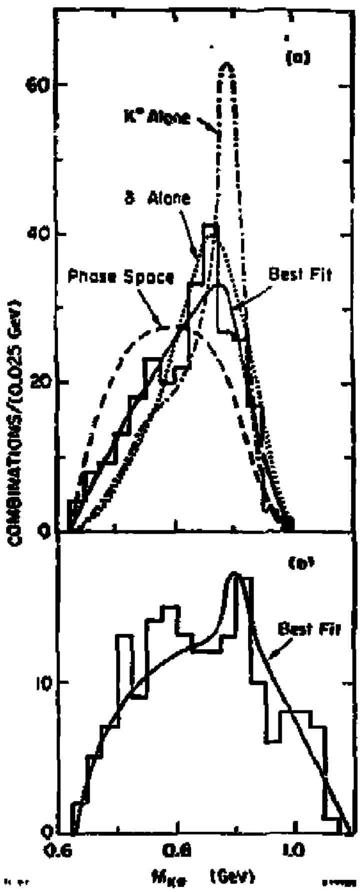

Fig. 17. Projections in $m_{K\pi^0}$ similar to Fig. 16.

complementary plots outside this region. Figure 16 shows that the fit needs a δ to achieve the low mass $K\bar{K}$ excess and Figure 17 shows that the fit cannot tolerate K^* alone, which causes too extreme a peak in $m_{K\pi}$. Both curves show that a significant change in shape occurs in the $K\bar{K}\pi$ mass region adjacent to the ι. The conclusion to which all of this analysis points is that the $\iota(1440)$ is a 0^- state decaying mainly via $\delta\pi$. As stated in Table II, the branching ratio product is

$$B(\psi \to \gamma\iota)B(\iota \to K\bar{K}\pi) = (4.0 \pm .7 \pm 1.0) \times 10^{-3} ,$$

where the first error is statistical and the second is systematic. The decay $\iota \to \eta\pi\pi$, for which there was some indication in the preliminary data, has not yet been quantified in the present sample. It might be expected from the decay $\delta \to \eta\pi$, but the information on δ decays is not definitive enough to permit a meaningful prediction.

Crystal Ball Results on $\psi \to \gamma\theta(1640)$

A search for gg bound states decaying into $\eta\eta$ was begun immediately following Bjorken's suggestion.[13] After accumulation of the sample of ψ discussed above, an effect was visible in the channel $\psi \to 5\gamma$, a 3C fit. Figure 18 shows the invariant mass of any two γ's plotted against the invariant mass of any two others (15 combinations per event). Signals corresponding to $\psi \to \gamma\eta\eta$ and $\psi \to \gamma\pi^0\pi^0$ are seen, with a large background that is mainly combinatorial. The 5γ events are fit to the hypothesis $\psi \to \gamma\eta\eta$ (5C) and the invariant mass of $\eta\eta$ is displayed (Figure 19). An enhancement emerges at a mass of 1640 MeV with a large but uncertain intrinsic width of 220^{+100}_{-70} MeV. Table III

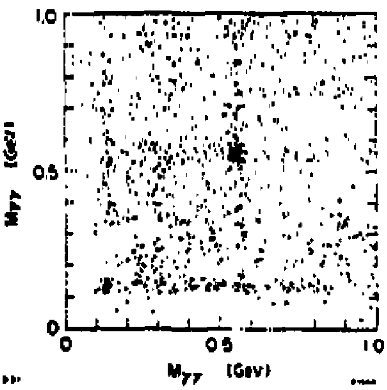

Fig. 18. Scatterplot of $m_{\gamma\gamma}$ vs $m_{\gamma\gamma}$ for all fifteen combinations of γ's from $\psi \to 5\gamma$ (Crystal Ball data).

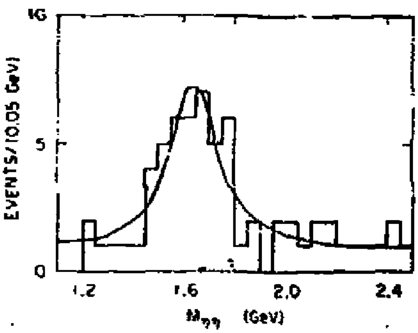

Fig. 19. The invariant mass spectrum of $\eta\eta$ pairs from fitted Crystal Ball events of the type $\psi \to \gamma\eta\eta$. The solid curve is the sum of a Briet-Wigner term and a small constant background term.

illustrates that although the precision in the energy of the photon and the fitted mass are very similar to the case for the $\iota(1440)$, the natural width of this object dominates the expected width of the transition γ-line in the inclusive γ spectrum. This broadening makes it harder to see, and indeed we see no clear evidence of this state in the total inclusive sample (Figure 13) unless it corresponds to the broad excess to the left of the visible $\iota(1440)$ peak. The inclusive γ distribution of 5γ events alone also shows no peaking at the expected k_γ = 1113 MeV, but the $\eta\eta\gamma$ mode is expected to be statistically inundated by background.

We have named this candidate state $\theta(1640)$ in a thinly veiled attempt to acknowledge the acuity of the motivator of the search, and as the only rational alternative to the unacceptable name B/J.

The state has been searched for in other channels, with no substantial result. In the channel $\psi \to \pi^0\pi^0$, where the dominant $\pi^0\pi^0$ effect is at $f^0(1270)$, there is a suggestion of an effect at 1640 (Figure 20). Interpreting all the events above f^0 in this region as signal leads to an upper limit $BR(\psi \to \gamma\theta)\ BR(\theta \to \pi\pi) < 6 \times 10^{-4}$, which is clearly not restrictive given that $BR(\psi \to \gamma\theta)BR(\theta \to \eta\eta) = (4.9 \pm 1.4 \pm 1) \times 10^{-4}$ is found in the other channel.

A spin-parity analysis of the $\psi \to \gamma\eta\eta$ events has been made.[28] Pose statist. s restrict the low value spin states to 0^+ or 2^+. The three independent angles used in the fitting procedure are shown in Figure 21. The procedure was verified by applying it to the $\psi \to \gamma f^0 \to \gamma\pi^0\pi^0$ state, where it excludes spin 0 by an enormous

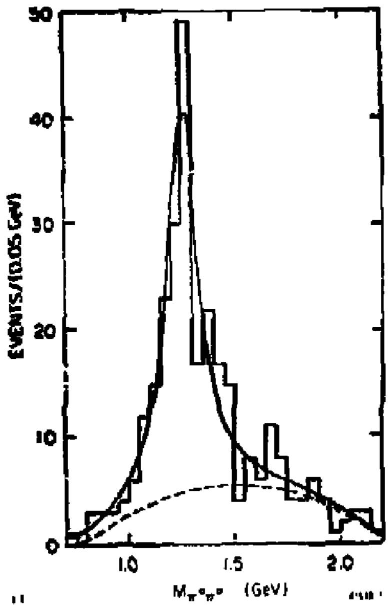

Fig. 20. The mass spectrum of $\pi^0\pi^0$ from fitted Crystal Ball events, including the most common ones where the π^0 is not distinguishable as 2 γ's and thus does not appear in the previous set $\psi \to 5\gamma$.

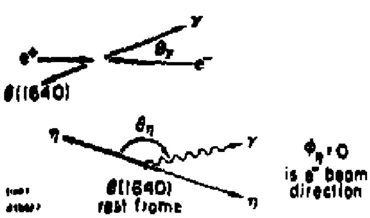

Fig. 21. Definition of angles used in the spin-parity analysis of the θ(1640).

factor; we note that much of the significance of this exclusion was developed from the fitted $\theta_\gamma - \theta_\eta - \phi_\eta$ correlations. The same procedure applied to $\psi \to \gamma\theta$ yields the result that

$$\frac{\text{Probability } (\theta \text{ is spin } 0)}{\text{Probability } (\theta \text{ is spin } 2)} = .045$$

plus some constraints on parameters of the spin 2 angular distribution. This two standard deviation result may also come from correlation effects, but it appears that an extremum of the $\cos\theta_\eta$ distribution suffices to explain the preference for spin 2. (Figure 22, $|\cos\theta_\eta| \approx 1$). This result makes the spin determination somewhat less compelling; a cleaner determination must await more data.

Plausible Theoretical Interpretations of the New States

The establishment of a bound state of two gluons would impose severe restrictions on the dynamics of QCD; it is thus prudent to examine alternatives to this interpretation of ι and θ. Table IV lists only a few

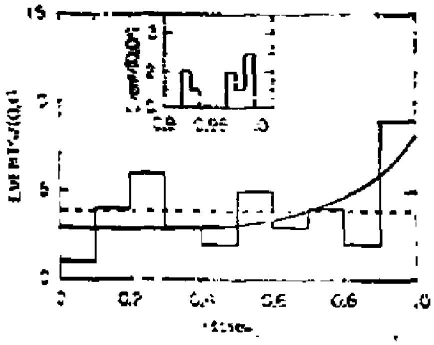

Fig. 22. Projection of the 3-dimensional angular distribution onto the θ axis. The dashed line is the distribution expected for spin-0, the solid line for spin-2. These expectations include the effects of finite resolution and detector efficiency. The inset shows the distribution within the bin, .9 to 1.0.

candidate theories in which 0^{-+} and 2^{++} (or 0^{++}) objects appear, but even these few show the intrinsic ambiguity of their assignment.

In the Jaffe and Johnson bag model,[26] the ι would be their 0^{-+} glueball predicted at 1290 MeV, while the θ could serve as either of their 2^{++} glueballs predicted at 980 and 1590 MeV, or as the similar mass 0^{++} objects (if we ignore our preliminary spin determination). The bag (Jaffee)[27] also predicts $q\bar{q}q\bar{q}$ objects: a 2^{++} at 1650 MeV and a 0^{++} at 650 MeV; we cannot exclude these.

The physically appealing model (valence gluons paired by color magnetism) of Cho, et al.,[28] predicts a 0^{-+} ($^3P_0$) state which can be adjusted to fit ι(1440) exactly but then has only 60% gluonic content. The prediction for the 2^{++} ($^5S_2$) glueball also has a free parameter but is expected with mass 1.7-2.0 GeV, a broad width of ~ 100 MeV and 80% gluonic content. In this scheme the 0^{++} ($^1S_0$) glueball might be the $S^*(980)$. This theory mixes the $q\bar{q}$ and gg resonances markedly and has specific predictions for the ratios of $\psi \to (q\bar{q})\gamma$ and $\psi \to (gg)\gamma$ for particles of similar spin-parity.

Finally, an alternative explanation for ι is as a radial excitation of $q\bar{q}$, from which Cohen and Lipkin[29] predict 0^{-+} objects at 1280 and 1500 MeV.

Table IV by no means exhausts the possibilities for assignments, but even so the experimenters have an unenviable task: they must find candidates for <u>all</u> hypothesized nonglueball states and

TABLE IV
Plausible Theoretical Interpretations
of the New States in ψ-decay.

State 0^{++}

Model	Bag, Jaffe & Johnson	Color $\mathcal{M}$, Cho et al.	Bag, Jaffee
Nature of State	$(TE)^2$ or $(TM)^2$ glueball	$^1S_0$ glueball	$q\bar{q}q\bar{q}$
Predicted Mass and % glue	960 or 1590; 100%	980; 70%	650; 0%
Correspondence	?	S*(980)?	?

State 0^{-+}

Model	Bag, Jaffe & Johnson	Color $\mathcal{M}$, Cho et al.	Cohen & Lipkin
Nature of State	(TE)(TM) glueball	$^3P_0$ glueball	$q\bar{q}$ radial excitation
Predicted Mass and % glue	1290 100%	tuned to 1440; 58%	(a) 1280; (b) 1500; 0% 0%
Correspondence	ι(1440)?	ι(1440)?	(a) $\eta\pi\pi$(1275)?, Stanton (b) ι(1440)?

State 2^{++}

Model	Bag, Jaffe & Johnson	Color $\mathcal{M}$, Cho et al.	Bag, Jaffe
Nature of State	$(TE)^2$ or $(TM)^2$ glueball	$^5S_2$ glueball	$q\bar{q}q\bar{q}$
Predicted Mass and % glue	960 or 1590; 100%	~ 1700 (Γ ~ 100) 80%	1650; 0%
Correspondence	θ(1640)?	θ(1640)?	θ(1640)?

have a few candidates left over, or must resort to poorly predicted values of masses, widths and relative branching ratios to try to eliminate incorrect theories. The appearance of these strong ψ radiative transitions, as predicted only for glueballs, must remain the most compelling feature of these data.

VI. FUTURE DIRECTIONS

Resolution of the above dilemmas lies in multiple directions of research.

(A) More data on $\psi \to \gamma X$ must be gathered to affirm the 2^{++} assignment for the $\theta(1640)$ and to look for more candidates.

(B) A search for different exclusive decay modes of the states already found should be made, in present and future data.

(C) A better understanding of the background and systematics of the inclusive γ distribution from ψ, especially for high-x γ's, would aid in extracting the predicted branching ratios ι/η, η'/η, θ/f, f'/f that would constrain many models.

(D) A precise measurement of $\Upsilon \to \gamma X$ should be made to see if there is the predicted recurrence of the set of states seen in $\psi \to \gamma X$. A second appearance of this strange assortment (by $q\bar{q}$ standards) would be a powerful argument that the set is a direct result of sampling the color singlet state of two gluons.

ACKNOWLEDGMENTS

I would like to thank my colleagues close to these works for their patient discourses on their analyses: D. G. Aschman, G. Gaiser, K. Königsman, F. C. Porter and D. L. Scharre. I also thank T. DeGrand for his repeated urgings that Crystal Ball data be examined for glueball effects and many detailed discussions of what these might be.

REFERENCES

1. Members of the Crystal Ball Collaboration. California Institute of Technology, Physics Department: C. Edwards, R. Partridge, C. Peck and F. Porter. Harvard University, Physics Department: A. Antreasyan, Y. F. Gu, W. Kollmann, M. Richardson, K. Strauch, K. Wacker and A. Weinstein. Princeton University, Physics Department: D. Aschman, T. Burnett (visitor), M. Cavalli-Sforza, D. Coyne, M. Joy, C. Newman and H. Sadrozinski. Stanford Linear Accelerator Center: E. D. Bloom, F. Bulos, R. Chestnut, J. Gaiser, G. Godfrey, C. Kiesling, W. Lavender, W. Lockman, J. Loffler, S. Lindgren, S. Lowe, M. Oreglia and D. Scharre. Stanford University, Physics Department and High Energy Physics Laboratory: D. Gelphman, R. Hofstadter, R. Horisberger, I. Kirkbride, H. Kolanoski, K. Koenigsmann, R. Lee, A. Liberman, J. O'Reilly, A. Osterheld, B. Pollock and J. Tompkins.
2. R. Partridge et al., Phys. Rev. Lett. 44, 712 (1980); Y. Chan et al., IEEE Trans. on Nucl. Sci., Vol. NS-25, No. 1, 333 (1978); I. Kirkbride et al., IEEE Trans. on Nucl. Sci., Vol. NS-26, No. 1, 1535 (1979).
3. E. D. Bloom, Proceeding of the 1979 International Symposium on Lepton and Photon Interactions at High Energies, August 23-29, 1979, Fermilab; SLAC-PUB-2425 (1979); R. Partridge et al., Phys. Rev. Lett. 45, 1150 (1980).
4. F. C. Porter, Proceedings of SLAC Summer Institute on Particle Physics, to be published as SLAC-PUB-2796 (1981); C. Edwards et al., SLAC-PUB-2814 (1981).
5. W. Bartel et al., Phys. Lett. 79B, 492 (1978).
6. M. Oreglia, Ph.D. thesis, Stanford University, SLAC Report 236 (1980).
7. K. Wilson, Phys. Rev. D10, 2445 (1974); H. Fritzsch and P. Minkowski, Nuovo Cimento 30A, 393 (1975); P. Freund and Y. Nambu, Phys. Rev. Lett. 34, 1645 (1975); J. Kogut and L. Susskind, Phys. Rev. 16, 395 (1975); K. Johnson, Phys. Lett. 60B, 201 (1976).
8. M. Chanowitz, Phys. Rev. D12, 918 (1975).
9. L. Okun and M. Voloshin, ITEP-95 (1976).
10. S. Brodsky, T. DeGrand, R. Horgan and D. Coyne, Phys. Lett. 73B, 203 (1978).
11. The above argument in this particular form was pointed out by D. Scharre (Ref. 25).
12. K. Koller and T. Walsh, Nucl. Phys. B140, 449 (1978), and DESY preprint 77/68.
13. J. D. Bjorken, Proceedings of SLAC Summer Institute on Particle Physics, SLAC Report 224 (1980).
14. J. S. Whitaker, Ph.D. thesis, U.C. Berkeley, LBL-5518 (1976).
15. C. Biddick et al., Phys. Rev. Lett. 38, 1324 (1977).
16. P. Moore, Sr. thesis, Princeton University, Department of Physics, April 1978 (unpublished); D. Coyne, notes of the 1979 Caltech QCD Workshop (unpublished).

17. M. Ronan, notes of the 1979 Caltech QCD Workshop (unpublished); L. Galtieri, Proceedings of the 14th Rencontre de Moriond, Les Arcs, France (March 1979); M. Ronan et al., Phys. Rev. Lett. 44, 367 (1980).
18. D. Scharre, Proceedings of the X International Symposium on Multiparticle Dynamics, Goa, India, September 1979 (published in 1980); G. Feldman, Proceedings of the 15th Rencontre de Moriond, Les Arcs, France (March 1980); G. Abrams et al., Phys. Rev. Lett. 44, 114 (1980); D. Scharre, Phys. Rev. D23, 43 (1981).
19. Unpublished presentations by J. Tompkins, SLAC (July 1979), D. Coyne, SFSU (November 1979), H. Kolanowski, SLAC (November 1979), T. Burnett, U.C. Irvine (December 1979); D. Aschman, SLAC-PUB-2550 (1980).
20. D. Scharre et al., Phys. Lett. 97B, 329 (1980).
21. D. Aschman, Proceedings of the 15th Rencontre de Moriond, Les Arcs, France (March 1980).
22. K. Ishikawa, Phys. Rev. Lett. 46, 978 (1981); M. Chanowitz, Phys. Rev. Lett. 46, 981 (1981); J. Donoghue et al., Phys. Lett. 99B, 416 (1981).
23. The candidate $(gg)_{1440}$ is termed G by M. Chanowitz, GBS by K. Ishikawa and ι by D. Scharre.
24. C. Dionisi et al., Nucl. Phys. B169, 1 (1980).
25. D. Scharre, SLAC-PUB-2801 (1981), to be published in the Proceedings of the 1981 International Symposium on Lepton and Photon Interactions at High Energies, Bonn, Germany, August 24-29, 1981.
26. R. Jaffe and K. Johnson, Phys. Lett. 60B, 201 (1976).
27. R. Jaffe, Phys. Rev. D15, 267,281 (1977), and Phys. Rev. D17, 1444 (1978).
28. Y. Cho et al., PAR/LPTHE 81/08, paper submitted to 1981 International Symposium on Lepton and Photon Interactions at High Energies, Bonn, Germany, August 24-29, 1981.
29. I. Cohen and H. Lipkin, Nucl. Phys. B151, 16 (1979).